

RESEARCH ARTICLE

Electrochemical investigation of the new dyad of the Zn²⁺ derivative of *meso*-5-(4-hydroxyphenyl)-10, 15, 20- tris (4-methoxy phenyl) porphyrin and *meso*-5-(4-hydroxyphenyl)-10,15,20-trisphenyl porphyrin points to photoinduced electron transfer

Ajith C. Herath^{1*}, Veranja Karunaratne², R.M.G. Rajapakse² and Anura Wickramasinghe²

¹ Department of Physical Sciences, Faculty of Applied Sciences, Rajarata University of Sri Lanka, Mihintale.

² Department of Chemistry, Faculty of Sciences, University of Peradeniya, Peradeniya.

Revised: 30 November 2011 ; Accepted: 03 January 2012

Abstract: The synthesis of a porphyrin dyad with the combination of free-base and Zn porphyrin units was attempted. The criterion for the selection of individual units was their monomer redox potentials. In this respect, several porphyrin derivatives, namely *meso*-5-(4-hydroxyphenyl)-10,15,20-trisphenyl porphyrin (HPTTrPP), *meso*-5-(4-hydroxyphenyl)-10, 15, 20- tris(4-methoxy phenyl) porphyrin (HPTTrMPP), *meso*-5-(4-hydroxyphenyl)-10,15,20-tris(4-sulfonatophenyl) ammoniumporphyrin [NH₄]₃[HPTTrSPP] and their Zn²⁺ derivatives were synthesized and characterized by UV-visible spectroscopy, ¹H NMR spectroscopy and cyclic voltammetry. Out of the six compounds, Zn²⁺ derivative of HPTTrMPP was found to show the lowest excited state oxidation potential (-1.41 V) while [NH₄]₃[HPTTrSPP] exhibited the lowest reduction potential of its ground state (-0.91 V) and that of the excited state at 0.94 V. Similarly, HPTTrPP also showed favourable one electron reduction potentials of -1.11 V and 0.77 V for ground and excited states, respectively. The coupling of Zn²⁺ derivative of HPTTrMPP (donor) and HPTTrPP (acceptor) was accomplished by means of a butyl spacer to yield the dyad. The excitation of ZnHPTTrMPP by visible light resulted in photoinduced electron transfer from ZnHPTTrMPP to HPTTrPP.

Keywords: Acceptor, donor, photoinduced electron transfer, porphyrin dyad.

INTRODUCTION

Porphyrin-based supramolecular architectures have been developed as a result of improved knowledge and the use of new synthetic strategies, along with sensitive instrumentation for the characterization of various physicochemical parameters of porphyrins. In this respect, recent discoveries on bridge mediated electronic

coupling in porphyrin based donor/bridge/acceptor systems enabled the construction of efficient photo-electronic systems to convert light into electrochemical energy (Osuka *et al.*, 1993, 1996, 2000; Andreasson *et al.*, 2000; D'Souza *et al.*, 2002; Imahori *et al.*, 2002; Takai *et al.*, 2010). These porphyrin assemblies represent stable models of the chlorophylls of green plants and bacterial light harvesting systems, where absorbed light is converted into chemical energy by vectorial photo induced electron transfers. The existence of a long-lived charge separated state, which in turn depends on the stabilization of the charge separation, which prevents charge recombination, is a key requirement in achieving the high efficiency in this important event (Liu & Bolton, 1992; Dijk *et al.*, 1996), which could be described, as the potential energy surfaces of the initial and final states of the charge separation process in the Marcus theory (Marcus & Sutin, 1985). An efficient stepwise approach for the construction of porphyrin arrays for mimicking the two key steps of photosynthesis, which are the light energy harvesting and photoinduced charge separation has been developed (Jensen *et al.*, 1997; Baraka *et al.*, 1998; Kajanus *et al.*, 1999; Kilsa *et al.*, 1999).

In the present study, a porphyrin dyad consisting of a metallo porphyrin unit acting as a donor and a free base porphyrin unit acting as an electron acceptor was synthesized. The two units were coupled by a saturated hydrocarbon spacer. The criterion for the selection of donor and acceptor units was based on the redox potentials of synthesized porphyrin monomers.

* Corresponding author (herath037@yahoo.com)

METHODS AND MATERIALS

Pyrrole, propanoic acid, benzaldehyde, *p*-hydroxybenzaldehyde, *p*-methoxybenzaldehyde (Sigma-Aldrich), chlorosulfonic acid, 1,4-dibromobutane (Alfa chemicals), anhydrous sodium sulfate, potassium carbonate (analytical grade, BDH) and tetraethylammonium tetrafluoroborate (Sigma-Aldrich) were used as received. All solvents, methanol, dichloromethane and chloroform were purified and dried according to standard methods (Perrin *et al.*, 1980) prior to use. The nuclear (¹H) magnetic resonance spectra were recorded on a 300 NMR spectrometer using D₂O or DMSO-*d*₆ as the solvent. The UV-visible spectra were recorded on a Shimadzu UV-visible spectrophotometer. The concentrations of the porphyrins used were in the range of 2.0×10^{-6} mol dm⁻³ (to observe the Soret band) to 5.0×10^{-5} mol dm⁻³ (to observe Q bands).

All cyclic voltammetric measurements were made in a conventional three-electrode voltammetric cell consisting of a glassy carbon working electrode, a Ag/AgCl wire as a quasi reference electrode and a Pt wire as the counter electrode. Voltage sweeping was done with a potentiostat (Oxford Instruments) and the current-potential curves were recorded on a BAS X-Y recorder (USA). Cyclic voltammograms were recorded for novel porphyrins in CH₂Cl₂ or CH₂Cl₂/CH₃OH (4:1) solvent mixture, in the presence of 0.1 mol dm⁻³ tetraethylammonium tetrafluoroborate as the supporting electrolyte. The solutions were degassed by nitrogen prior to each electrochemical experiment. The concentration of each porphyrin used was 1.0×10^{-3} mol dm⁻³.

Synthesis of porphyrin monomers:

meso-5-(4-hydroxyphenyl)-10,15,20-trisphenyl porphyrin (HPTTrPP) - compound 1: Pyrrole (2.68 g, 40 mmol) was added to refluxing propanoic acid (300 mL) containing benzaldehyde (3.16 g, 30 mmol) and *p*-hydroxybenzaldehyde (1.34 g, 1.1 mmol). The mixture was refluxed for 1 h and left over-night at room temperature. The propanoic acid was removed under reduced pressure, leaving a black-violet residue. The product was washed with hot water, air dried and chromatographed on basic alumina using CHCl₃:CH₃OH (95:5 V/V) mixture as the eluant. Evaporation of the solvent under reduced pressure yielded 0.25 g (10%) of the crystalline violet coloured product. UV/vis (CH₂Cl₂): λ_{max}/nm 418, 515, 550, 590, 648. ¹H NMR (300 MHz in CDCl₃, δ in ppm): 8.84 (m, 8H, pyrrole β-H), 8.20 (m, 8H, phenyl *o*-H), 7.75 (m, 8H, phenyl *m*, *p*-H), -2.84 (br s, 2H, imino H).

meso-5-(4-hydroxyphenyl)-10, 15, 20- tris (4-methoxyphenyl) porphyrin (HPTrMPP) - compound 2: Pyrrole (5.37 g, 80 mmol) was added to refluxing propanoic acid (500 mL) containing *p*-methoxybenzaldehyde (8.33 g, 60 mmol) and *p*-hydroxybenzaldehyde (2.44 g, 20 mmol). The mixture was refluxed for 1 h and left over-night at room temperature. Propanoic acid was removed under reduced pressure, leaving a black-violet residue. The product was washed with hot water, air-dried and chromatographed on basic alumina using CHCl₃. The fast moving small maroon coloured band, comprising the tetra substituted porphyrin product followed by a green impurity band was discarded. The main product was isolated using CHCl₃: CH₃OH (95:5 V/V) mixture as the eluant. Evaporation of the solvent under reduced pressure yielded 0.25 g (12 %) of the violet coloured product. UV/vis (CH₂Cl₂): λ_{max}/nm 419, 518, 552, 593, 650. ¹H NMR (300 MHz in CDCl₃, δ in ppm): 8.84 (m, 8H, pyrrole β-H), 8.01–8.12 (m, 8H, phenyl *o*-H), 7.52 (m, 8H, phenyl *m* -H), 4.08 (s, 9H, -OCH₃) -2.65 (br s, 2H, imino H).

meso-5-(4-hydroxyphenyl)-10, 15, 20- tris (4-sulfonatophenyl) ammonium porphyrin [NH₄]₃[HPTrSPP] - compound 3: The porphyrin HPTrPP (0.98 g, 1.55 mmol) was dissolved in CHCl₃ (150 mL) in a 250 mL three neck flask. Chlorosulfonic acid (7.04 g, 4.0 mL) was slowly added with vigorous stirring and the mixture was heated for 2 h at 45 °C under a nitrogen atmosphere. The stirring was continued until the evolution of HCl gas ceased. Excess chlorosulfonic acid was decomposed by the addition of ice-cold water (100 mL). The mixture was kept at 5 °C for 3 h and filtered. The precipitate was dissolved in dry methanol (100 mL) and ammonia gas was passed through the solution until its green colour changed to red. The volume of the solution was reduced to 20 mL and dry acetone (60 mL) was added to precipitate the sulfonated porphyrin. The solution was filtered and the product was obtained as a black-violet compound: yield 72%. UV/vis (CH₃OH): λ_{max}/nm 415, 513, 548, 589, 645. ¹H NMR (300 MHz in CDCl₃/CD₃OD, δ in ppm): 8.88 (m, 8H, pyrrole β-H), 8.26 (m, 8H, phenyl *o*-H), 7.78 (m, 8H, phenyl *m*-H), -2.81 (br s, 2H, imino H).

Zn derivative of compounds 1, 2 and 3: The free base porphyrins (60 mg) of compounds 1, 2 and 3, were separately dissolved in a mixture of CH₃OH:CHCl₃ (50 mL), a two-fold excess of zinc acetate in CH₃OH (3.0 mL) was added and the mixture was refluxed for 2 h. The progress of the reaction was monitored by recording the absorption spectra. After the metallation was completed, the reaction mixture was reduced to a small volume and poured into a beaker containing water. The mixture was extracted with CHCl₃ and dried over

anhydrous Na_2SO_4 . Evaporation of the solvent gave almost quantitative (> 90%) yield of the desired Zn(II) porphyrin.

Synthesis of porphyrin dimer - compound 4: The zinc derivative of compound 2 (31 mg, 0.04 mmol) and 25 mg (0.04 mmol) of compound 1 were added to a solution of 1,4-dibromobutane (0.1 mL, 0.84 mmol) in 100 mL of dry acetone. The mixture was refluxed, in the presence of 0.1 g of anhydrous K_2CO_3 for 24 h. After the removal of acetone under reduced pressure the residue was chromatographed on neutral alumina with CH_2Cl_2 as the eluant. The first yellow band was the impurity and the two separated maroon coloured bands, which followed contained the two porphyrin compounds. After evaporation of the solvent, the first fraction yielded 40% violet coloured $\text{H}_2\text{P}-\text{H}_2\text{P}$. UV/vis (CH_2Cl_2): $\lambda_{\text{max}}/\text{nm}$ 420, 515, 550, 550, 648. ^1H NMR (300 MHz in CDCl_3 , δ in ppm): 8.82–8.87 (m, 16H, pyrrole β -H), 8.20 (m, 16H, phenyl *o*-H), 7.75–7.72 (m, 22H, phenyl *m,p*-H), 4.25 (m, 4H, $-\text{OCH}_2$), 3.61 (m, 4H, $-\text{CH}_2\text{CH}_2-$), -2.75 (s, 2H, imino H). The second fraction yielded 31% violet coloured $\text{ZnP}-\text{H}_2\text{P}$. UV/vis (CH_2Cl_2): $\lambda_{\text{max}}/\text{nm}$ 421, 550, 609. ^1H NMR (300 MHz in CDCl_3 , δ in ppm): 8.82–8.87 (m, 16H, pyrrole β -H), 8.20 (m, 16H, phenyl *o*-H), 7.75–7.72 (m, 22H, phenyl *m,p*-H), 4.25 (m, 4H, $-\text{OCH}_2$), 3.61 (m, 4H, $-\text{CH}_2\text{CH}_2-$), -2.75 (s, 2H, imino H).

RESULTS AND DISCUSSION

^1H NMR spectral data of porphyrins

The strong ring π -electronic current of the macrocyclic core characterizes the position of the proton signal in the ^1H NMR spectra of porphyrin. Therefore, typically NH protons appear as a singlet up field due to shielding effects of ring currents in the range from -1.5 to -4.0 ppm. However, NH protons, when an acidic proton moiety is attached to *meso* position of the porphyrin ring show fast proton exchange reaction resulting a low intense broad singlet at -2.8 ppm. The signals of pyrrole β -protons average out and appears from 8.5 to 9.5 ppm.

UV-visible spectral data of porphyrins

The electronic absorption spectrum of a free-base porphyrin consists of a highly intense Soret band owing to a strong transition to the second excited state ($S_0 \rightarrow S_2$) at about 400 nm and a weak transition to the first excited state ($S_0 \rightarrow S_1$) around at 550 nm (Q-band). Both bands arise due to $\pi-\pi^*$ transitions and the weak long-wavelength Q band consists of four peaks (Figures 1 & 2). In contrast, the four peaks in Q-band of free-base porphyrins, metalloporphyrins exhibit only two absorption peaks in

the Q-band due to the higher symmetry of the molecule (Figures 2 & 3).

Cyclic voltammetry of synthesized porphyrins

In order to investigate the electron donor and acceptor properties of the synthesized porphyrins at ground state and excited states, cyclic voltammetric experiments were carried out to estimate ground state redox potentials.

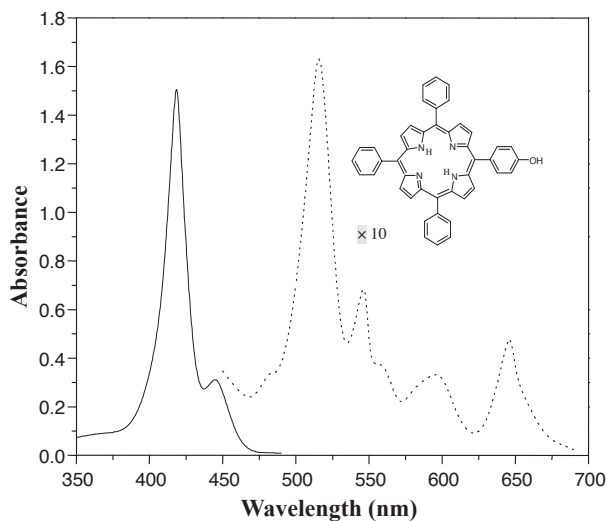


Figure 1: UV-visible spectrum of *meso*-5-(4-hydroxyphenyl)-10,15,20-trisphenyl porphyrin in methanol. Soret band (—), Q-band (.....) at 298 K

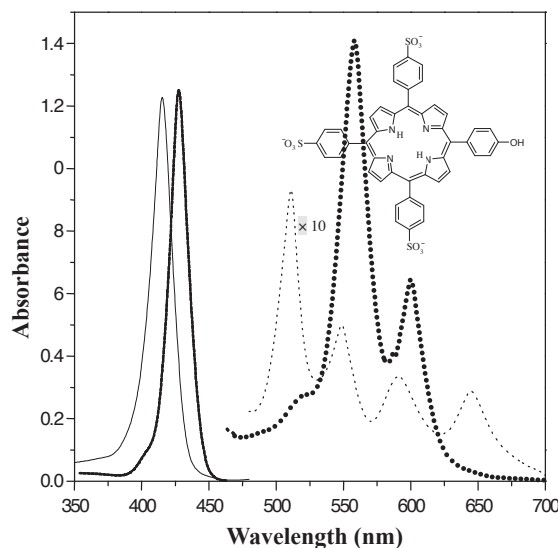


Figure 2: UV-visible spectra of $[\text{NH}_4]_3[\text{HPTrSPP}]$, Soret band (—), Q-band (.....) and its Zn(II) analogue in methanol, Soret band (—), Q-band (.....)

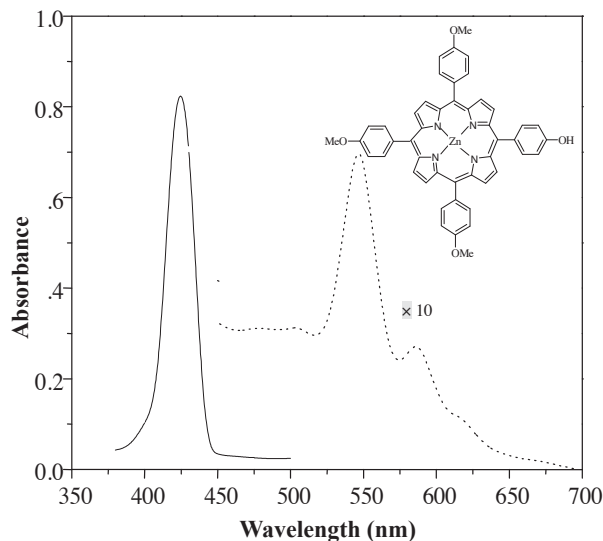


Figure 3: UV-visible spectrum of Zn(II)HPTTrMPP in methanol. Soret band (—), Q-band (.....)

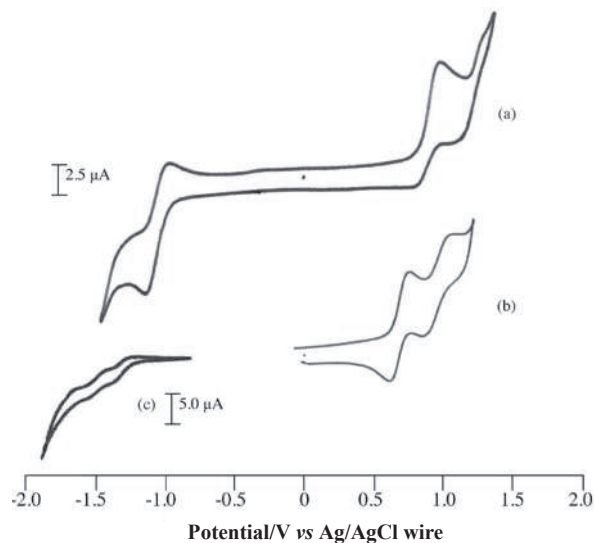


Figure 4: Cyclic voltammograms of HPTTrPP (a) and ZnHPTTrPP (b) in CH_2Cl_2 at a glassy carbon electrode under N_2 saturation. Scan rate 50 mV s^{-1} . Voltammogram recorded for ZnHPTTrPP at a scan rate of 20 mV s^{-1} (c). Supporting electrolyte is 0.1 mol dm^{-3} tetraethylammoniumtetra fluoroborate

Basically, porphyrins show ring-based and metal-centered redox reactions in voltammetry (Felton & Linschitz, 1966; Christopher *et al.*, 1988). Ring-centered potentials are much more dependent on the hetero atom of the porphyrin core due to change in energies of the highest occupied molecular orbital (HOMO) and the lowest unoccupied molecular orbital (LUMO). As the electronegativity of the hetero atom increases, the ground state potential and thereby the excited state oxidation potential increases while the reduction potential decreases. Therefore, thioporphyrins (one or more pyrrole rings are replaced by thiophene ring/s) are better oxidants and poorer reductants in both ground and excited states than ordinary porphyrins (Pandian & Chandrashekar, 1993). The nature of the central metal ion significantly affects the relative energy level distribution of the metal x^2-y^2 orbital and the empty porphyrin e_g (π^*) orbital, which in turn determines the addition of the first electron to the metal ion or the ring (Srinivasan *et al.*, 1999).

The cyclic voltammograms (CVs) of the free base and zinc porphyrins in CH_2Cl_2 are depicted in Figure 4. The voltammogram of free base HPTTrPP consists of a well-defined reversible redox couple ($E_{p1/2} = -1.06 \text{ V}$, $I_{pc}/I_{pa} \approx 1$), a quasi-reversible couple ($\Delta E_p = 130 \text{ mV}$) and an irreversible oxidation at 1.30 V . The first oxidation reaction of ZnHPTTrPP occurs at a less positive potential

(0.78 V) compared to that of HPTTrPP (0.98 V) due to the inductive effect of the central Zn(II) metal ion. The electron density of the porphyrin ring is increased by π -back donation from metal to the porphyrin ring, making it more susceptible to oxidation. It follows that the oxidation of the porphyrin ring becomes easy when the central metal ion is more electropositive (Kim *et al.*, 2001).

The cyclic voltammetric responses of HPTTrMPP and ZnHPTTrMPP (Figure 5) exhibit two ring oxidations at potentials 0.6 V , 0.91 V and 0.56 V , 0.91 V , respectively. At negative potentials, CVs show a quasi-reversible redox couple at $E_{1/2} = -1.0 \text{ V}$ and an irreversible peak at -1.14 V corresponding to the addition of the first electron to the ring of HPTTrMPP and its Zn derivative, respectively. The decrease in oxidation potentials (Figure 5b) for these compounds ($E_{pa} = 0.6 \text{ V}$ and $E_{pa} = 0.56 \text{ V}$) and substantial increase in oxidation potential for the compound $[\text{NH}_4]_3[\text{HPTTrSPP}]$ ($E_{pa} = 1.14 \text{ V}$) are depicted in voltammograms (Figure 5c).

This indicates that the nature of the phenyl substituent at the *meso* position has some influence on the redox reactions taking place in the macrocyclic ring. As the CVs illustrate, electron donating substituent ($-\text{OCH}_3$) favours ring oxidation while electron withdrawing substituent ($-\text{SO}_3^-$) makes ring oxidation difficult.

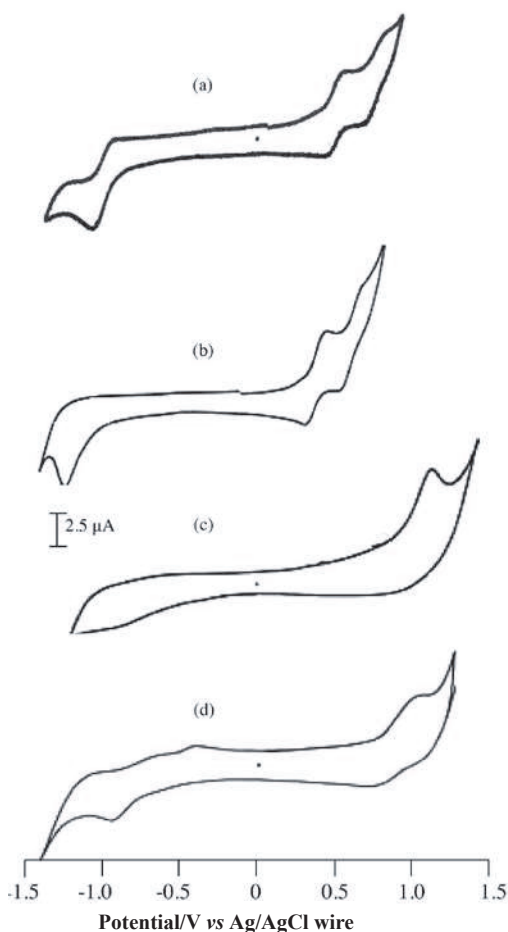


Figure 5: Cyclic voltammograms of HPTTrMPP (a) ZnHPTTrMPP (b) in CH_2Cl_2 and HPTTrSPP (c), ZnHPTTrSPP (d) in $\text{CH}_2\text{Cl}_2/\text{CH}_3\text{OH}$ at a glassy carbon electrode under N_2 saturation. Scan rate 50 mV s^{-1} . Supporting electrolyte is 0.1 mol dm^{-3} tetraethylammonium tetrafluoroborate

Table 1 shows the redox potentials of porphyrins in their ground states, as well as excited states. The excited state potential was calculated using the following equation.

$$E [D^+/D^*] = E [D^+/D] - \Delta H (D^*, D) + T\Delta S (D^*, D)$$

Where E is the excited state potential of the electron donor (D) and ΔH and ΔS are the enthalpy and entropy changes between the excited state and the ground state of the molecule.

It is reported that in condensed phase, the enthalpy difference between excited and ground state of the same molecule is practically equal to the zero-zero spectroscopic energy (E^{0-0}) of the excited state. The entropy difference, which arises due to changes in dipole moment, internal degrees of freedom, orbital and spin degeneracy is negligible for most practical systems (Scandole & Balzani, 1983).

The excited energy (S_1), estimated for all these compounds are between 1.85 – 2.00 eV . Their cyclic voltammograms have one oxidation peak in the range of 0.50 V to 1.15 V and a reduction peak in the range of -0.90 to -1.35 V . From the absorption onset, the absorption energy corresponding to the π - π^* transition for each compound was calculated. Combining these data with the ground state redox potentials, the excited state redox potentials were calculated. These data show that, ZnHPTTrMPP has the most negative excited state potential (-1.41 V) for P^{*+}/P^* couple and hence is the most anodic material in its excited state. Conversely, ZnHPTTrSPP has the most positive P^*/P^{*-} excited state potential (1.06 V) making it the best cathodic material in its excited state. The coupling of the two compounds would then enable an electron transfer from the former to the latter from their excited states making a charge-separated couple.

Table 1: Ground state and singlet excited state redox potentials of porphyrins in CH_2Cl_2

Compound	E^{0-0}/eV	$E_{\text{Ox}}(P/P^{*+})$	$E_{\text{Red}}(P/P^{*-})$	$E_{\text{Ox}}(P^*/P^{*+})$	$E_{\text{Red}}(P^*/P^{*-})$
HPTTrPP	1.88	0.98	-1.11	-0.87	0.77
Zn HPTTrPP	2.00	0.78	-1.34	-1.22	0.66
HPTTrMPP	1.90	0.60	-1.14	-1.30	0.76
ZnHPTTrMPP	1.97	0.56	-1.14	-1.41	0.83
[HPTTrSPP] $^{3-}$	1.85	1.14	-0.91	-0.71	0.94
[ZnHPTTrSPP] $^{3-}$	2.00	1.04	-0.94	-0.96	1.06

According to the redox potentials listed in Table 1, ZnHPTTrMPP and HPTrPP could also be used as anodic and cathodic materials, respectively to construct a donor-acceptor couple. The two units were coupled by a saturated hydrocarbon spacer. The first compound isolated in the purification process shows a sharp singlet at 2.75 ppm for four ring NH protons (a broad weak singlet for starting materials) in the ^1H NMR spectrum indicating that phenolic OH in the starting materials are no longer available due to the formation of a spacer linkage in the dyad. The protons of $-\text{OCH}_2-$ resonate as a multiplet at 4.25 ppm and four equivalent protons of $-\text{CH}_2\text{CH}_2-$ of the spacer resonate at 3.6 ppm.

The absorption spectra obtained for the dyad $\text{H}_2\text{P}-\text{H}_2\text{P}$ (Figure 6) exhibited an identical pattern of peaks to that of recorded for HPTrPP. ^1H NMR data along with absorption spectral data thus indicated that the dyad is composed of two monomer units of HPTrPP and therefore, the following structure could be proposed for

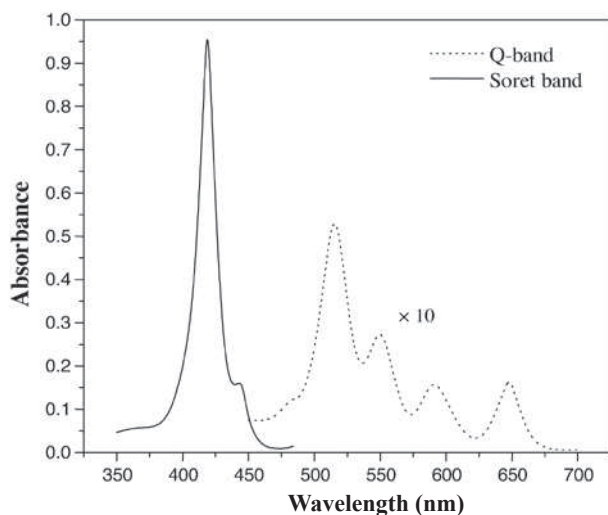


Figure 6: UV-visible spectrum of porphyrin dyad ($\text{H}_2\text{P}-\text{H}_2\text{P}$) in CH_2Cl_2 at 298 K

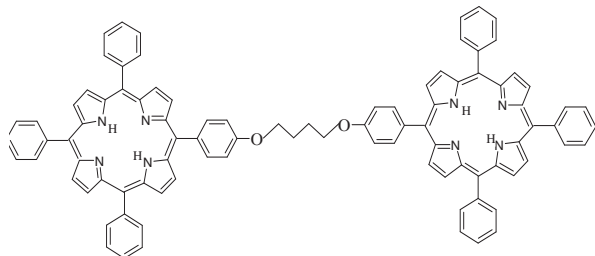


Figure 7: The structure of the porphyrin dyad ($\text{H}_2\text{P}-\text{H}_2\text{P}$)

the dyad (Figure 7). In the dyad, H_2P and ZnP refer to the free base and metallated porphyrins respectively.

The ^1H NMR spectrum of the second fraction isolated in the purification process shows the disappearance of the peak around $\delta -2.7$ ppm indicating that one of the porphyrin moieties is holding a Zn^{2+} ion. Such a structure was supported by its absorption spectrum, which exhibited a reduced number of peaks (Figure 8) compared to that of a free base porphyrin. Further, metallation of this dyad with zinc acetate gave a different absorption spectrum resembling that of ZnHPTTrMPP (Figure 9), indicating that the original dyad is partially metallated ($\text{H}_2\text{P}-\text{ZnP}$).

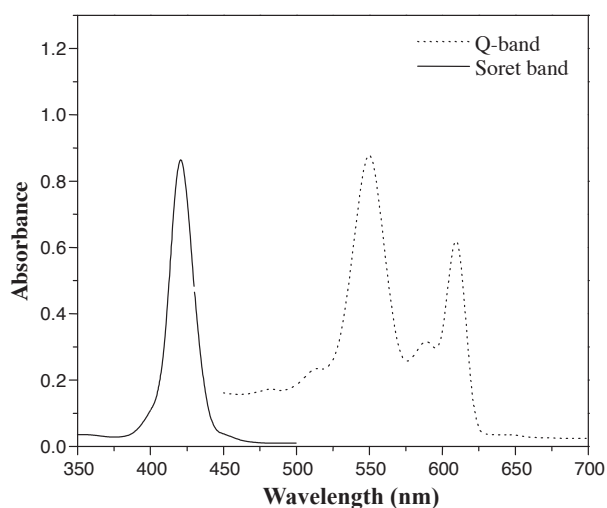


Figure 8: UV-visible spectrum of porphyrin dyad ($\text{ZnP}-\text{H}_2\text{P}$) in CH_2Cl_2

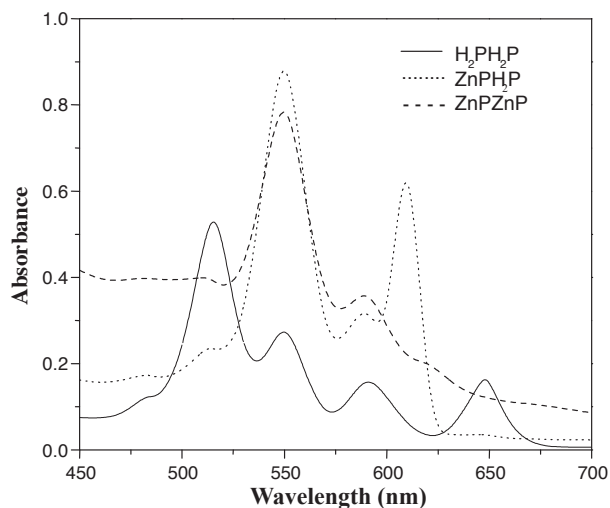


Figure 9: Absorption spectra of some porphyrin dyads in CH_2Cl_2

The cyclic voltammogram of ZnP-H₂P in dichloromethane exhibits two well-defined redox couples at $E_{p_{1/2}} = 0.75$ V and $E_{p_{1/2}} = 1.03$ V in the anodic region and a quasi reversible couple at $E_{p_{1/2}} = -1.27$ V in the cathodic region (Figure 10). The potential of the first anodic redox couple of ZnP-H₂P is the same as that of ZnHPTrMPP and the reduction potential (-1.32 V) is little less in comparison to that of ZnHPTrMPP (-1.37 V). Based on all available data, it is reasonable to propose the following structure (Figure 11) for the metallated dyad.

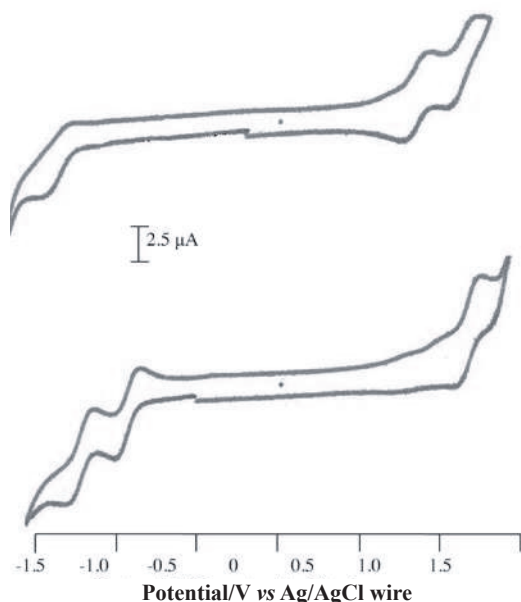


Figure 10: Cyclic voltammograms of ZnP-H₂P (top) and H₂P-H₂P (bottom) in CH₂Cl₂ at glassy carbon electrode under N₂ saturation. Scan rate 50 mV s⁻¹. Supporting electrolyte is 0.1 mol dm⁻³ tetraethylammonium tetrafluoroborate

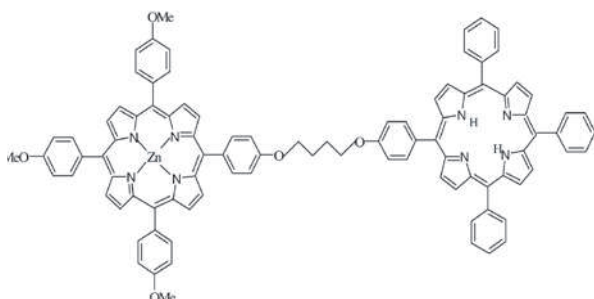


Figure 11: The structure of the ZnP-H₂P dyad

CONCLUSION

A porphyrin dyad with one metal-centered unit having low oxidation potential (donor) and a freebase unit with low reduction potential (acceptor) facilitates photoinduced electron transfer from electron donor to electron acceptor. In this dyad, no considerable change in redox potentials and absorption spectral data were observed compared to the corresponding monomer units, which could be due to lack of π conjugation between the two units.

REFERENCES

1. Andreasson J., Kajanus J., Martensson B. & Albinsson. (2000). Triplet energy transfer in porphyrin dimers: comparison between δ - and δ' -chromophore bridged systems. *Journal of the American Chemical Society* **122**: 9844–9845.
2. Baraka M.E., Janot J.M., Ruhlmann L., Giraudeau A., Deumie M. & Seta P. (1998). Photoinduced energy and electron transfers in the porphyrin triad (zinc octaethylporphyrin - 4,4' bipyridinium - tetraphenylporphyrin)²⁺, 2 ClO₄⁻). *Journal of Photochemistry and Photobiology A: Chemistry* **113**: 163–169.
3. Brett C.M.A. & Brett A.M.C.F.O. (1988). The influence of the halide electrolyte on the electrochemical reduction pathway of some meso-tetrasubstituted porphyrin free bases in N,N-dimethyl formamide. *Journal of Electroanalytical Chemistry* **255**: 199–213.
4. Christopher M.A., Ana Maria C.F. & Brett O. (1988). The influence of the halide electrolyte on the electrochemical reduction pathway of some meso-tetrasubstituted porphyrin free bases in NJV-dimethyl formamide. *Journal Electroanalytical Chemistry* **255**: 199–213.
5. D'Souza F., Deviprasad G.R., Zandler M.E., Hoang V.T., Klykov A., VanStipdonk M., Perera A., El-Khouly M.E., Fujitsuka M. & Ito O. (2002). Spectroscopic, electrochemical, and photochemical studies of self-assembled *via* axial coordination Zinc porphyrin-fulleropyrrolidine dyads. *The Journal of Physical Chemistry A* **106**: 3243–3252.
6. Felton R.H. & Linschitz H. (1966). Polarographic reduction of porphyrins and electron spin resonance of porphyrin anions. *Journal of the American Chemical Society* **88**: 1113–1116.
7. Imahori H., Tamaki K., Araki Y., Hasobe T., Ito O., Shimomura A., Kundu S., Okada T., Sakata Y. & Fukuzumi S. (2002). Linkage dependent charge separation and charge recombination in porphyrin-pyromellitimide-fullerene triads. *The Journal of Physical Chemistry A* **106**: 2803–2814.
8. Jensen K.K., van Berlekom S.B., Kajanus J., Martensson J. & Albinsson B. (1997). Mediated energy transfer in covalently linked porphyrin dimers. *The Journal of Physical Chemistry A* **101**(12): 2218–2220.

9. Kajanus J., van Berlekom S.B., Albinsson B. & Martensson J. (1999). Synthesis of bis(phenylethynyl)arylene-linked diporphyrins designed for studies of intramolecular energy transfer. *Synthesis–Stuttgart* **7**: 1155–1162.
10. Kilsa K., Kajanus J., Martensson J. & Albinsson B. (1999). Mediated electronic coupling: singlet energy transfer in porphyrin dimers enhanced by the bridging chromophore. *The Journal of Physical Chemistry B* **103**: 7329–7339.
11. Kim J., Rhee S. W., Na Y. H., Lee K. P., Do Y. & Jeoung, S. C. (2001) X-ray structure and electrochemical properties of ferrocene-substituted metalloporphyrins *Bulletin of Korean Chemical Society* **22**(12): 1316–1322.
12. Liu J.Y. & Bolton R. (1992). Intramolecular photochemical electron transfer. 7. Temperature dependence of electron-transfer rates in covalently linked porphyrin-amide-quinone molecules. *The Journal of physical chemistry* **96**(4): 1718–1725.
13. Marcus R. & Sutin N. (1985). Electron transfers in chemistry and biology. *Biochimica et Biophysica Acta* **811**: 265–322.
14. Osuka A., Marumo S., Mataga N., Taniguchi S., Okada T., Yamazaki I., Nishimura Y., Ohno T. & Nozaki K. (1996). A stepwise electron-transfer relay mimicking the primary charge separation in bacterial photosynthetic reaction center. *Journal of the American Chemical Society* **118**(1): 155–168.
15. Osuka A., Nakajima S., Maruyama K., Mataga N., Asahi T., Yamazaki I., Nishimura Y., Ohno T & Nozaki K. (1993). 1,2-Phenylene-bridged diporphyrin linked with porphyrin monomer and pyromellitimide as a model for a photosynthetic reaction center: synthesis and photoinduced charge separation. *Journal of the American Chemical Society* **115**: 4577– 4589.
16. Osuka A., Noya G., Taniguchi S., Okada T., Nishimura Y., Yamazaki I. & Mataga N. (2000). Energy gap dependence of photoinduced charge separation and subsequent charge recombination in 1,4-phenylene-bridged zinc-free base hybrid porphyrins. *Chemistry: A European Journal* **6**(1): 33–46.
17. Osuka A., Yamada H., Maruyama K., Mataga N., Asahi T., Ohkouchi M., Okada T., Yamazaki I. & Nishimura Y. (1993). Synthesis and photoexcited-state dynamics of aromatic group-bridged carotenoid-porphyrin dyads and carotenoid-porphyrin-pyromellitimide triads. *Journal of American Chemical Society* **115**(21):9439–9452.
18. Pandian R.P. & Chandrashekar T.K. (1993). Water-soluble thiaporphyrins and metallothiaporphyrins; synthesis, characterization, ground- and excited-state properties. *Journal of the Chemical Society, Dalton Transactions* **1993**: 119–125.
19. Perrin D.D., Perrin D.R. & Armarege W.L.F. (1980). *Purification of Laboratory Chemicals*, 2nd edition. Pergamon Press, Oxford, UK.
20. Scandola F. & Balzani V. (1983). Energy-transfer processes of excited states of coordination compounds. *Journal of Chemical Education* **60**: 814–823.
21. Srinivasan A., Pushpan S.K., Kumar M.R., Mahajan S., Chandrashekar T.K., Roy R. & Ramamurthy P. (1999). Meso-Aryl sapphyrins with heteroatoms; synthesis, characterization, spectral and electrochemical properties. *Journal of the Chemical Society, Perkin Transactions 2*: 961–968.
22. Takai A., Chkounda M., Eggenpiller A., Gros C.P., Lachkar M., Barbe J. & Fukuzumi S. (2010). Efficient photoinduced electron transfer in a porphyrin tripod-fullerene supramolecular complex via π - π Interactions in Nonpolar Media. *Journal of the American Chemical Society* **132**: 4477– 4489.
23. van Dijk S.I., Groen C.P., Hartl F., Brouwer A.M. & Verhoeven J.W. (1996). Long-lived triplet state charge separation in novel piperidine-bridged donor-acceptor systems. *Journal of the American Chemical Society* **118**: 8425–8432.